European Journal of Pharmaceutics and Biopharmaceutics 131 (2018) 99–108

Contents lists available at ScienceDirect

European Journal of Pharmaceutics and Biopharmaceutics

journal homepage: www.elsevier.com/locate/ejpb

Research paper

Formulation and *in vitro* evaluation of a siRNA delivery nanosystem decorated with gH625 peptide for triple negative breast cancer theranosis

Sanaa Ben Djemaa[a], Stephanie David[a,*], Katel Hervé-Aubert[a], Annarita Falanga[b], Stefania Galdiero[b], Emilie Allard-Vannier[a], Igor Chourpa[a], Emilie Munnier[a]

[a] EA6295 Nanomédicaments et Nanosondes, Université de Tours, 31 Avenue Monge, 37200 Tours, France
[b] Department of Pharmacy, CIRPEB – University of Naples "Federico II", Via Mezzocannone 16, 80134 Napoli, Italy

ARTICLE INFO

Keywords:
SPION
Chitosan
Poly-L-arginine
Cell-penetrating peptide
Nanovector
Down-regulation

ABSTRACT

The development of an efficient small interfering RNA (siRNA) delivery system has held scientists interest since the discovery of the RNA interference mechanism (RNAi). This strategy gives hope for the treatment of many severe diseases. Herein, we developed hybrid nanovectors able to deliver siRNA to triple negative breast cancer cells. The nanovectors are based on PEGylated superparamagnetic iron oxide nanoparticles (SPION) functionalized with gH625 peptide, chitosan and poly-L-arginine. Every component has a key role and specific function: SPION is the core scaffolding the nanovector; PEG participates in the colloidal stability and the immune stealthiness; gH625 peptide promotes the nanovector internalization into cancer cells; cationic polymers provide the siRNA protection and favor siRNA endosomal escape and delivery to cytosol. The formulation was optimized by varying the amount of each compound. The efficacy of the siRNA retention and protection were investigated in the presence of high concentration of serum. Optimized nanovectors show a high uptake by MDA-MB-231 cells. The resulting down regulation of GFP expression was 73 ± 3% with our nanovector compared to 59 ± 8% obtained with the siRNA-Oligofectamine™ complex in the same conditions.

1. Introduction

Triple negative breast cancer (TNBC) is classified as one of the most aggressive forms of breast cancer and is generally associated with high tumor grade and a poor survival. TNBC is characterized by the absence of estrogen receptor, progesterone receptor and human epidermal growth factor receptor 2 [1]. The lack of these receptors deprives the TNBC of the benefits of specific therapy targeting these proteins [2]. That is one of the reasons why no effective targeted therapy is available for TNBC and its treatment presents a major clinical challenge [3]. To combat this disease and to reduce female mortality, novel approaches have to be developed.

One promising strategy which has provided hope for the treatment of various severe diseases like cancer is based on the use of small interfering RNA (siRNA) [4–6]. This strategy emerged after the demonstration of the mechanism of RNA interference (RNAi) in mammalian cells in 2001 [7]. SiRNA are double-stranded RNA of 21–25 nucleotides in length, which act with specificity on post-transcriptional gene extinction. SiRNA have a high ability to recognize complementary mRNAs and to guide the associated cytosolic RNA-induced silencing complex (RISC). This association leads to the mRNA degradation and consequently the inhibition of gene expression [8]. For cancer treatment, this strategy is used to induce the down-regulation of genes coding for proteins implicated in cancer cells proliferation and tumor growth [9]. However, when siRNA are administrated in systemic circulation there are some limitations. Indeed, the negative charge of siRNA limits their ability to cross cell membranes and the presence of enzymes in the blood, such as ribonucleases, affects siRNA stability and leads to their rapid degradation [10]. Consequently, it is necessary to develop a delivery system to protect siRNA, prolong their blood

Abbreviations: SiRNA, small interfering RNA; RNAi, RNA interference; SPION, superparamagnetic iron oxide nanoparticles; PEG, polyethylene glycol; GFP, green fluorescent protein; TNBC, triple negative breast cancer; CPP, cell-penetrating peptide; CS-FNP, CPP-capped stealth fluorescent nanoparticles; CS-MSN, CPP-capped stealth magnetic siRNA nanovectors; N, amine groups; P, phosphate groups; Cs, chitosan; PLR, poly-L-arginine; MR, mass ratio; N_{CS}/P, the molar ration of the positive charges of chitosan amine groups and the negative charges of siRNA's phosphate groups; N_{PLR}/P, the molar ration of the positive charges of poly-L-arginine amine groups and the negative charges of siRNA's phosphate groups; HD, hydrodynamic diameter; PDI, polydispersity index; ZP, zeta potential; FBS, fetal bovine serum; SiGFP, siRNA anti-GFP; SiCtrl, non-targeted siRNA

* Corresponding author.
E-mail address: stephanie.david@univ-tours.fr (S. David).

https://doi.org/10.1016/j.ejpb.2018.07.024
Received 18 April 2018; Received in revised form 24 July 2018
Available online 29 July 2018

circulation time, improve their bioavailability, allow their internalization by target cells and intracytoplasmic siRNA release.

One strategy is to associate siRNA with nanocarrier systems to effectively deliver the therapeutic siRNA towards their target [11,12]. In this context, superparamagnetic iron oxide nanoparticles (SPION) appear as a suitable candidate thanks to their safety for *in vivo* application. In fact, SPION are already used as contrast agents for magnetic resonance imaging (MRI) [13] and they are prevalently used in the development of nanocarriers for siRNA delivery [4,14–16]. In our team, we previously synthesized fluorescent SPION coated with polyethylene glycol (PEG) polymer and functionalized with the cell-penetrating-peptide (CPP) gH625 [17]. In the present paper, we will name these nanoparticles CS-FNP (as CPP-capped stealth fluorescent nanoparticles). The CS-FNP labeling with Cyanine 5.5 covalently attached to the SPION core allows to monitor them in cells and tissues using fluorescence. The PEG shell around SPION improves their colloidal stability and stealthiness [18,19]. The membranotropic gH625 peptide [20] conjugated to the PEG shell of the nanoparticles is intended to promote their uptake into cells. Due to their small size below 100 nm and their nearly neutral zeta potential, the CS-FNP appeared appropriate for intravenous (i.v) injection. CS-FNP showed a prolonged colloidal stability in biological medium and an efficient uptake by MDA-MB-231 cancer cells [17].

In this work, we used the CS-FNP nanoplatform to develop a magnetic siRNA nanovector called CS-MSN (as CPP-capped stealth magnetic siRNA nanovector) for triple negative breast cancer theranosis (Fig. 1).

Cationic polymers like chitosan carrying amino groups (NH_3^+, hereafter named N) are often formulated with poly-anionic siRNA carrying phosphate groups (PO_4^{3-}, hereafter named P), in order to protect the latter against degradation and promote internalization into cells [16,21,22]. Moreover, thanks to their buffering capacity and their action as “proton sponges”, cationic polymers escape from endosomes and thus can enhance the passage of siRNA to the cytosol [23]. Our CS-MSN included two cationic polymers: chitosan (hereafter called Cs) and poly-L-arginine (hereafter called PLR). Cs is known for its large use in siRNA delivery due to its safety, biocompatibility and biodegradability [24]. Several studies demonstrated the role of Cs in siRNA delivery and transfection efficiency [15,21,22]. The ability of polyarginine to bind anionic siRNA and to complex them with other components of nanovectors (such as other polymers and/or iron oxide nanoparticles) has been also reported and largely exploited in the development of siRNA delivery nanosystems [16,25].

First, the CS-MSN formulation was optimized by varying the N/P ratio of the different polymers. Then, the CS-MSN stability in biologically relevant conditions, their toxicity and the siRNA transfection efficiency were evaluated.

2. Materials and methods

2.1. Preparation of cell-penetrating peptide stealth magnetic siRNA nanovector

2.1.1. Synthesis of CPP-capped stealth-fluorescent nanoparticles (CS-FNP)

The synthesis of CS-FNP is based on a protocol previously published by our group [17]. Briefly, to obtain these nanoparticles, SPION were silanized, labeled with cyanine 5.5, PEGylated in their surface and then functionalized with gH625 peptide. After the functionalization we modified the purification protocol by performing a dialysis (MWCO 300KDa) against PBS at 4 °C and in the dark for around 6 h, while PBS in the acceptor volume was changed every 1 h. CS-FNP were finally concentrated by Vivaspin® (cut-off of 30 kDa, Fisher Scientific, Illkirch, France).

2.1.2. Formulation of CPP-capped stealth-magnetic siRNA nanovectors (CS-MSN)

The formulation of CS-MSN is based on a protocol developed by David *et al.* and previously published by our laboratory [26]. Briefly, CS-MSN were formulated by loading siRNA and cationic polymers, chitosan (Cs, MW 110–150 kDa; degree of acetylation: ≤ 40 mol.%) and poly-L-arginine (PLR, MW 15–70 kDa) (both from Sigma-Aldrich Chimie GmbH, St. Quentin Fallavier, France) into CS-FNP. On the one hand, siRNA were precomplexed with PLR, on the other hand CS-FNP were precomplexed with chitosan and then both precomplexes were mixed together to obtain CS-MSN. The siRNA loading was defined by the iron/siRNA w/w ratio (MR) of 10. The cationic polymers loading was defined as N/P ratio, i.e. the molar ratio of the positive charges of polymers and the negative charges of siRNA. In order to optimize the nanovectors, the Cs/siRNA relative content (hereafter called N_{CS}/P) was varied from 0 to 100. and the PLR/siRNA relative content (hereafter called N_{PLR}/P) was varied from 0 to 6.

2.2. Size and zeta potential analysis

The size, the polydispersity index (PDI) and the zeta potential (ZP) were determined using a Nanosizer apparatus (Zetasizer®, Malvern Instrument, UK). The measurements of hydrodynamic diameter (HD)

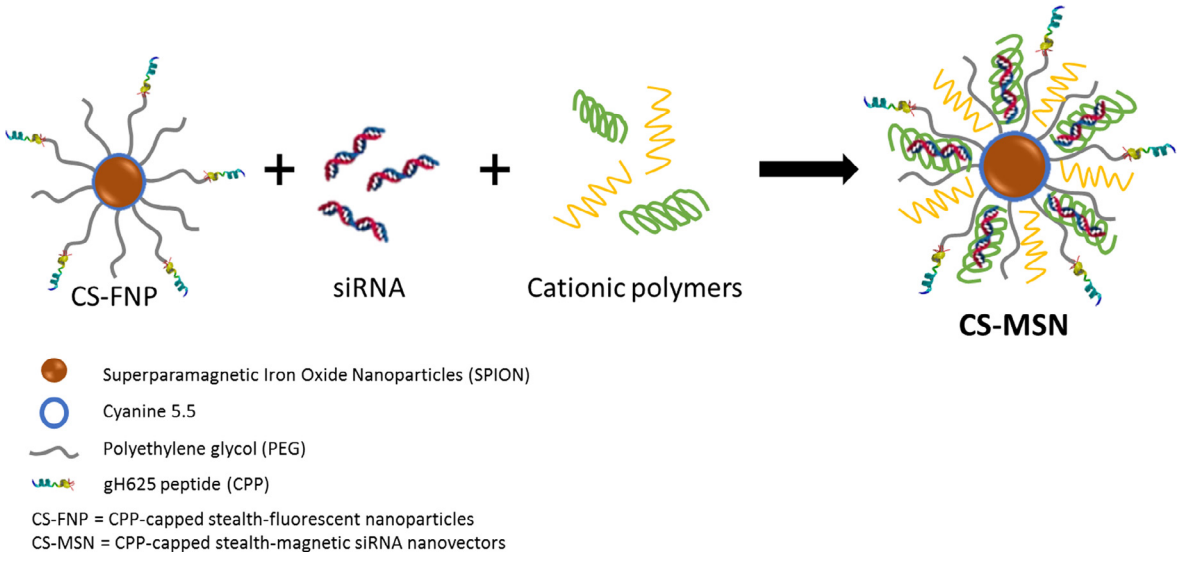

Fig. 1. Scheme of CS-MSN and its components, CS-FNP, siRNA and cationic polymers.

and zeta potential of CS-FNP (iron concentration of 50 mg/l) were performed in PBS 1X and $NaNO_3$ solution (0.01 M), respectively. For the CS-MSN, the HD and the ZP were obtained after dilution of CS-MSN in $NaNO_3$ 0.01 M (1:25 v/v) to fix the ionic strength. These measurements were achieved at 25 °C. The mean values of HD given were based on intensity. All measurements were made in triplicate and mean values ± SD were recorded.

2.3. Agarose gel electrophoresis and heparin decomplexation assay

Gel electrophoresis technique was used to verify the complexation of siRNA. Samples were prepared to deposit a content of 1.2 µM of siRNA per well. To release siRNA and control their integrity after formulation, heparin (Sigma-Aldrich Chemie GmbH, Steinheim, Germany) was added at a final concentration of 3 mg/ml. A loading buffer (Agarose gel loading dye 6X, Fisher, Bioreagents®, Illkirch, France) was added to all the samples before the deposit in wells. An agarose gel (1% m/v) was prepared containing 0.01% (v/v) ethidium bromide (EtBr) to visualize free siRNA. After deposition of the samples on the agarose gel, the migration was conducted in a Tris-acetate-EDTA (TAE) 1X buffer (Acros Organics, Geel, Belgium) for 15 min at 150 V. Free siRNA were visualized by UV-imaging using the EvolutionCapt software on a Fusion-Solo.65.WL imager (Vilbert Lourmat, Marne-la-Vallée, France). The fluorescence intensity of bands was quantified using Image J software.

2.4. Retention and protection in serum

To study the retention and the protection of siRNA in the presence of serum, CS-MSN or a solution of siRNA (2 µM) were added to an equal volume of a solution of Dulbecco's modified Eagle medium (DMEM) (Gibco®, Life Technologies, Paisley, UK) containing different percentages of fetal bovine serum (FBS) (Eurobio, Les Ulis, France) to obtain a final percentage of serum of 5%, 10% and 50%. After 4 h of incubation at 37 °C, gel retardation assay (as described in section 2.3) was performed.

2.5. Cell culture

Triple negative breast cancer cells MDA-MB-231 (a kind gift from the team MINT, UMR INSERM 1066 – CNRS 6021, University of Angers, France) and MDA-MB-231 stably expressing GFP (MDA-MB-231/GFP) (Euromedex, Souffelweyersheim, France) were maintained in DMEM supplemented with 10% fetal bovine serum, 1% non-essential amino acid (HyClone Laboratories, Logan, Utah) and 1% penicillin/streptomycin (Gibco®, Life Technologies, Paisley, UK) at 37 °C in an atmosphere containing 5% CO_2. Culture medium was changed every 48–72 h and the cells were harvested using trypsin/EDTA (0.05%) (Gibco®, Life Technologies, Paisley, UK) at 80% of confluency.

2.6. Transfection assay

One day before the transfection, MDA-MB-231/GFP cells were seeded at 3.10^4 cells/well in 12 well-plates. The day of transfection, CS-MSN and Oligofectamine™ (Invitrogen, Thermo Fisher Scientific, Paisley, UK) were prepared with anti-GFP siRNA at a final siRNA concentration of 50 nM according to the formulation protocol and the manufacture recommendation, respectively. Cells were treated with CS-MSN in equal parts of complete medium and Opti-MEM medium (Gibco®, Life Technologies, Paisley, UK) (1:1 v/v) and maintained in normal growth conditions for 30 min to 72 h or for 72 h with Oligofectamine™ (manufacture recommendation). Non-treated cells and cells transfected with CS-MSN loaded with a non-targeting siRNA sequence (siRNA Ctrl) were used as a negative control. Cells were removed using trypsin and then analyzed 24, 48 or 72 h after treatment using a FACSCalibur flow cytometer (BD Bioscience, Franklin Lakes, NJ). Data was analyzed using FlowJo v10 software. The percentage of gene silencing was calculated using the FL-1 median (median of the GFP fluorescence histogram).

2.7. Cytotoxicity

Cell viability was evaluated by a colorimetric assay based on the measurement of mitochondrial activity in viable cells using a stable tetrazolium salt WST-1 (Sigma Aldrich Chimie, St. Quentin Fallavier, France). MDA-MB-231 cells were seeded in 96 well-plate at 4.10^3 cells/well. After 24 h, cells were incubated with nanovectors prepared at different concentrations of siRNA (from 12.5 to 100 nM) for 4, 24 or 48 h. Then, the culture medium was replaced by a fresh complete medium containing 10% (v/v) WST-1 reagent for 3 h at 37 °C. Non-treated cells were used as a negative control while cells incubated with H_2O_2 at 20 mM were used as a positive control. The absorbance was measured at 450 nm using KC-junior V1.40 software on a BIO-TEK EL800 microplate reader. The number of viable cells is directly proportional to the absorbance value. The percentage of viable cells was calculated according to the followed equation:

$$Viability\,(\%) = \frac{As - Apc}{Anc - Apc} \times 100$$

As, Apc and Anc are, respectively, the absorbances of the sample, the positive control (H_2O_2) and the negative control (non-treated cells).

2.8. Internalization assay

Cellular internalization of CS-MSN by MDA-MB-231 cancer cells was evaluated by following the cyanine 5.5 fluorescence of CS-FNP using flow cytometry. MDA-MB-231 cells were seeded onto 6-well plates at 10^6 cells/well and were allowed to adhere for 24 h. CS-MSN were added to cells for 4 h after replacement of the complete cell culture medium by an equal part of complete medium and Opti-MEM medium (1:1 v/v). Non-treated cells were used as a negative control. Immediately after treatment, cells were washed and were removed using trypsin.

2.9. Statistics

Values were expressed as means ± standard deviations (SD). PRISM (GraphPad Prism 7) was used for statistical analysis. Data were compared among groups using Mann and Whitney test. The difference between groups was considered significant when p-value < 0.05 (*), < 0.01 (**) or < 0.001 (***).

3. Results and discussion

3.1. Development of an efficient CS-MSN formulation for siRNA delivery

3.1.1. Choice of poly-L-arginine for a complete siRNA complexation

The formulation of CS-MSN was based on the use of synthesized CS-FNP which had a size of 79 ± 8 nm and a zeta potential of −6 ± 1 mV. The first cationic polymer tested for CS-MSN development was chitosan. In order to obtain a CS-MSN formulation with a high transfection efficiency in cancer cells, we started by varying the molar ratio between the positive charges of chitosan amine groups and the negative charges of siRNA's phosphate groups (N_{CS}/P ratio). Fernandes and coworkers [27] used chitosan to siRNA weight ratio of 50:1 (the equivalent of N_{CS}/P ratio of 100:1) to completely complex siRNA with chitosan. In a study by Sun and colleagues [22], siRNA were complexed efficiently with PEG-chitosan at a weight ratio of PEG-CS to siRNA of 100:1. According to these results, the N_{CS}/P ratio was varied from 0 to 100. The second formulation parameter is the mass ratio (MR = iron mass of CS-FNP/siRNA mass) which was fixed at 10 for the following experiments, according to previously obtained results [26].

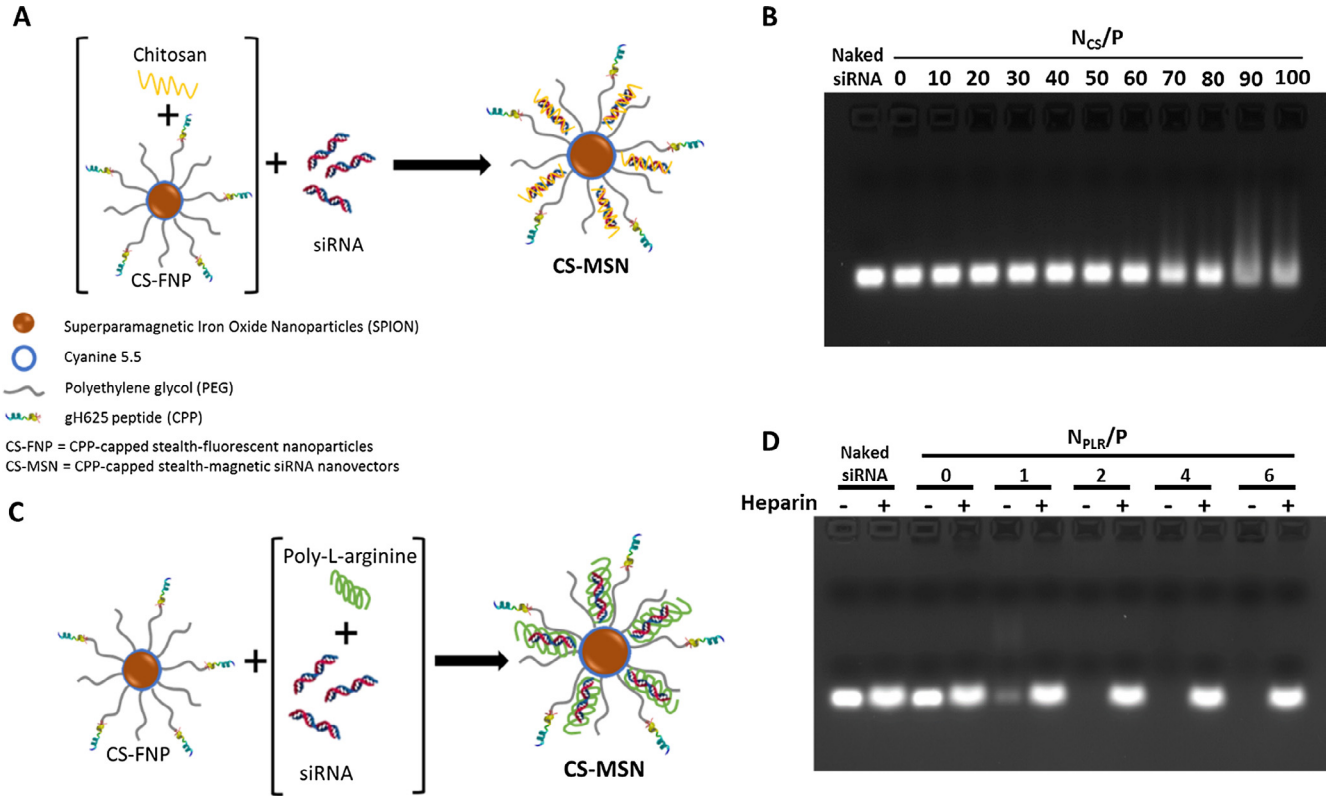

Fig. 2. Formulation of CS-MSN and detection of free siRNA in formulated CS-MSN. (A) Formulation scheme of CS-MSN prepared with CS-FNP, siRNA and chitosan. (B) Gel retardation assay to detect free siRNA in CS-MSN prepared with CS-FNP, siRNA and chitosan. (C) Formulation scheme of CS-MSN prepared with CS-FNP, siRNA and PLR. (D) Gel retardation assay to detect free siRNA in CS-MSN prepared with CS-FNP, siRNA and PLR, with (+) or without (−) heparin.

The formulation of CS-MSN was performed according to the following protocol: chitosan was firstly mixed with CS-FNP, then siRNA were added (Fig. 2. A). The siRNA retention in final complexes was evaluated using agarose gel retardation assay. After applying the electric field, free siRNA migrate and appear as fluorescent bands, while complexed siRNA remain in the loading wells. The fluorescence intensity is directly proportional to the quantity of free siRNA. As shown in Fig. 2B, the fluorescent bands, indicating free siRNA, were observed in all samples at different N_{CS}/P ratios. The fluorescence intensity seems to be reduced at a N_{CS}/P ratio higher than 80, but there is always more than 80% of free siRNA in the formulation. This result indicates that at these N_{CS}/P ratios chitosan was not able to promote complete siRNA complexation with CS-FNP.

In order to improve siRNA complexation, another highly cationic polymer, poly-L-arginine (PLR, pKa = 12) was investigated. PLR, similarly to chitosan, has a high capacity to complex negatively charged molecules like siRNA. The amount of PLR used in the formulation was defined, as for chitosan, using the N/P molar ration (N_{PLR}/P ratio). SiRNA were precomplexed with PLR at different N_{PLR}/P values from 0 to 6 and then added to CS-FNP (Fig. 2C). SiRNA retention was evaluated using agarose gel electrophoresis. To release siRNA and control their integrity after formulation, a heparin decomplexation assay was performed. As shown in Fig. 2D, the migration of siRNA was completely blocked from a N_{PLR}/P ratio of 2. In fact, without heparin, no fluorescent band was observed for samples prepared at N_{PLR}/P ≥ 2. However, when heparin was added, siRNA was released from the complexes, indicating that PLR can successfully complex the siRNA with the CS-FNP nanoparticles even at a low N_{PLR}/P ratio. In the literature, complexation efficiency of siRNA with polyarginine was already investigated. Zhao *et al.* demonstrated that polyarginine complexes siRNA from a N/P ratio of 10 in a study for the development of nanomicelles for siRNA delivery [16,25]. In another study, Veiseh *et al.* succeeded to completely condense siRNA with iron oxide nanoparticles coated with polyarginine at a weight ratio of 20 [16]. However, in our case, the N_{PLR}/P ratio for complete siRNA complexation are much lower than these reported.

The implication of CS-FNP in CS-MSN composed of CS-FNP, siRNA and PLR, was checked by performing a gel retardation assay of siRNA/PLR complexes (without CS-FNP), and it showed a total complexation of siRNA indicating that PLR is the major component which complex siRNA. The data for N_{PLR}/P = 2 are presented in Fig. S1. A, as at this N_{PLR}/P ratio all siRNA were complexed. Furthermore, the size and zeta potential of formulations prepared with siRNA and PLR with and without CS-FNP at N_{PLR}/P = 2 were measured (Fig. S1B and Table S1). Results indicated that CS-FNP improved the organization of siRNA and PLR and induced a more homogenous size distribution.

To choose the N_{PLR}/P ratio, the size and the surface charge of CS-MSN were measured as these parameters are two other important criteria to characterize when developing nanovector for siRNA delivery. As shown in Table 1, the addition of PLR increases the hydrodynamic diameter (HD) of the complexes to exceed 200 nm at N_{PLR}/P ratio of 6. The zeta potential remained lower than or equal to 0 mV up to N_{PLR}/P ratio of 6. It was previously reported that cellular uptake and biodistribution of nanoparticles is strongly affected by nanoparticles size. Indeed, large nanoparticles with diameters higher than 200 nm could stimulate immune system by activating the complement system [28]. As

Table 1
Hydrodynamic diameter (HD), polydispersity index (PDI) and zeta potential (ZP) of CS-MSN prepared with CS-FNP, siRNA and PLR.

	HD (nm)	PDI	ZP (mV)
N_{PLR}/P = 1	78 ± 7	0.34 ± 0.05	−7.3 ± 0.4
N_{PLR}/P = 2	143 ± 12	0.33 ± 0.04	−4.6 ± 0.3
N_{PLR}/P = 4	172 ± 9	0.26 ± 0.01	−2.1 ± 0.3
N_{PLR}/P = 6	255 ± 15	0.35 ± 0.01	0.3 ± 0.2

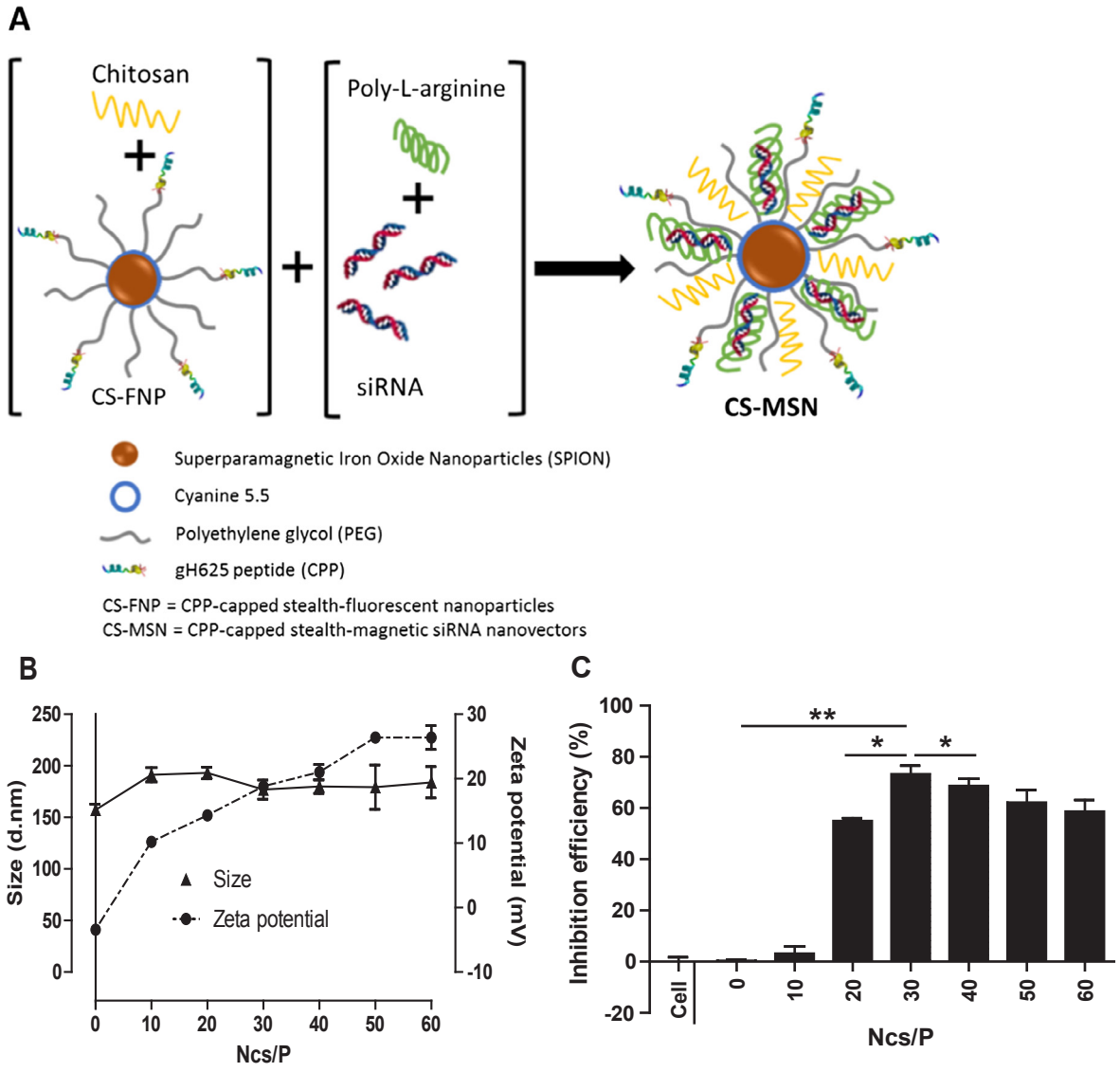

Fig. 3. Preparation and characterization of CS-MSN formulated with CS-FNP, siRNA, PLR and different amount of chitosan. (A) Formulation scheme of CS-MSN. (B) Hydrodynamic diameter and zeta potential. (C) Down regulation efficiency of GFP fluorescence in MDA-MB-231/GFP cells treated with CS-MSN prepared at MR = 10, $N_{PLR}/P = 2$ and at different N_{CS}/P ratio, siRNA/PLR ($N_{PLR}/P = 2$) and siRNA/PLR/CS ($N_{PLR}/P = 2$, $N_{CS}/P = 30$) complexes.

the size of complexes at $N_{PLR}/P = 6$ is higher than 200 nm, this N_{PLR}/P ratio was excluded from our choice. At $N_{PLR}/P = 1$, siRNA are not well complexed and to limit the quantity of PLR, we fixed the N_{PLR}/P at 2 for the following experiments. However, at this N_{PLR}/P ratio, the zeta potential of CS-MSN was rather negative, which could limit the internalization into cells. It was shown that positively charged nanoparticles are more internalized than negatively charged nanoparticles [29] and this could be explained by the increased electrostatic attraction between positive charges of nanoparticles and negative charged cell membrane.

3.1.2. Addition of chitosan for an efficient siRNA delivery

To add supplementary positive charges, which could promote the cellular entry of CS-MSN, we added chitosan (Fig. 3A), but we had to verify that it did not lead to an increase in the size beyond 200 nm. The size and the zeta potential of formulated CS-MSN formulated with N_{CS}/P ratios from 0 to 60 were measured (Fig. 3B) and the siRNA complexation was checked using gel electrophoresis (data not shown). Results indicate that the addition of chitosan to the formulation increased the hydrodynamic diameter of CS-MSN up to 170–190 nm. The polydispersity index (PDI) was around 0.3 for all formulations which is quite usual for formulations using electrostatic self-assembly. Moreover, the zeta potential increased gradually with the N_{CS}/P ratio up to 28 mV because of the increased amount of amino groups. Additionally, gel electrophoresis results show a total siRNA complexation at all tested N_{CS}/P ratios indicating that the addition of chitosan does not disturb the siRNA complexation with PLR and CS-FNP.

To select the N_{CS}/P ratio for an efficient siRNA delivery, a transfection assay was carried out. Therefore, MDA-MB-231/GFP cells were treated with CS-MSN containing anti-GFP siRNA (50 nM) and formulated at N_{CS}/P ratio from 0 to 60. Cells were analyzed using flow cytometry to measure the fluorescence intensity of GFP (Fig. 3C). Successful transfection of anti-GFP siRNA would result in reduced GFP fluorescence compared to non-transfected cells and would therefore indicate successful siRNA delivery. Without chitosan, no reduction in the GFP fluorescence intensity was observed compared to non-treated cells, indicating that CS-MSN failed to inhibit the GFP expression. When the N_{CS}/P ratio increased up to 30, the GFP fluorescence intensity decreased compared to non-treated cells indicating that the down regulation efficiency increased up to 73%. For higher N_{CS}/P ratios, the GFP fluorescence intensity seems to decrease less than for N_{CS}/P ratio of 30, indicating a decreased down regulation. Thus, the most efficient CS-

MSN were formulated at N_{CS}/P ratio of 30. These results indicate that even if chitosan is not involved in the complexation of siRNA into CS-MSN (Fig. 2B), it seems to be important to obtain a size less than 200 nm with a slightly positive zeta potential. Furthermore, flow cytometry result highlights the importance of chitosan for an efficient siRNA transfection. That suggest that chitosan plays a key role in the intracellular trafficking of the CS-MSN. Martens and coworkers demonstrated that chitosan has an important role in the endosomal escape [30] which is a crucial step for siRNA intracellular delivery. It was previously noted that the use of chitosan at a relatively high N/P ratio promote the compactness of the nanovector structure and led to smaller size compared to low N/P ratio [31]. Moreover, Liu et al. showed that a poor transfection efficiency is correlated to low N/P ratios. The greater knockdown efficiencies were observed with nanovectors formulated with chitosan at N/P ratios higher than 30, however cytotoxicity was recorded with formulations prepared at N/P ratios higher than 70 [32]. In this study, it appears that both polymers are complementary: PLR enables complete siRNA complexation (Fig. 2D) thanks to its high positive charge density, and chitosan improves the siRNA delivery and the transfection efficiency of CS-MSN (Fig. 3C). Taken these results together, we defined the optimal formulation parameters of CS-MSN with adequate characteristics and a high transfection efficiency in cancer cells at MR ratio of 10, N_{PLR}/P ratio of 2 and N_{CS}/P ratio of 30.

3.2. Characterization of the optimized CS-MSN formulation

3.2.1. Implication of CS-FNP in the CS-MSN formulation

To check if CS-FNP are included in final CS-MSN, the size of formulations prepared with siRNA, PLR and chitosan at $N_{PLR}/P = 2$ and $N_{CS}/P = 30$ were measured and compared with formulations including CS-FNP. Without CS-FNP, the complexes showed sizes higher than 200 nm, with a high standard deviation (36 nm). The addition of CS-FNP to the formulation reduced the size of the final complexes and their standard deviation to 175 ± 7 nm. Additionally, the polydispersity index, representing the size distribution within the sample, diminishes (Table 2) and the shape of the peak changed from a large peak to a well-defined peak with a maximum at 175 nm when CS-FNP are included (Fig. 4A and B). It seems that the presence of CS-FNP improved the organization of CS-MSN and induced a more homogenous size distribution. Moreover, the zeta potential decreased from +30.7 mV to +14.2 mV after the addition of CS-FNP, indicating also an implication of CS-FNP in the final CS-MSN. Furthermore, the implication of CS-FNP on the down regulation of GFP was checked by transfecting MDA-MB-231/GFP cells with these complexes (Fig. 4C). CS-MSN, including CS-FNP, appeared more efficient to transfect cells and to reduce the GFP expression, indicating the importance of CS-FNP in the formulation.

3.2.2. Retention and protection of siRNA in the presence of serum

The principal roles of the nanovector are the retention and the protection of siRNA in biological medium. Before moving to *in vitro* experiments, the ability of CS-MSN to provide these two needs, was studied in presence of cell culture medium containing different amount of serum (5–50%) and compared to non-formulated (naked) siRNA and CS-MSN or naked siRNA in water (Ctrl) (Fig. 5). Gel retardation assay shows that the fluorescence intensity of naked siRNA incubated with 5% and 10% of serum was reduced at 4 h compared to 0 h and Ctrl. Moreover, after 4 h of incubation in 50% of serum, the fluorescent band disappeared indicating that all siRNA are degraded (Fig. 5A). For CS-MSN, regardless of the serum amount and incubation time, no fluorescent band was observed in absence of heparin. In presence of heparin, fluorescent bands of CS-MSN incubated with serum were observed at a similar intensity to that of CS-MSN in water and to that of naked siRNA in water (Fig. 5B) demonstrating that siRNA were not degraded by enzymes in presence of serum. In the literature, the effect of chitosan and poly-L-arginine to protect siRNA loaded in nanocarriers has already been shown. For example, Sun and coworkers showed a good retention and protection of siRNA complexed with chitosan-PEG conjugate after incubation with 50% of serum for up to 12 h, even if there was a visible degradation between 8 h and 12 h [22]. Our results show a high serum-protection and siRNA retention in CS-MSN even after incubation for 4 h with a high concentration of serum (50%), which is largely superior to the one used in the following *in vitro* experiments (5%). Moreover, the complete release of siRNA by optimized CS-MSN observed immediately after the addition of heparin, reflects a good balance between serum-protection and siRNA release which present a desirable trait for siRNA transfection.

Table 2
Hydrodynamic diameter (HD), polydispersity index (PDI) and zeta potential (ZP) of complexes formed with siRNA, PLR and Cs and that of CS-MSN prepared with CS-FNP, siRNA, PLR and Cs.

	HD (nm)	PDI	ZP (mV)
SiRNA/PLR/Cs polyplex ($N_{PLR}/P = 2$, $N_{CS}/P = 30$)	213 ± 36	0.43 ± 0.05	30.7 ± 1.4
CS-MSN (MR = 10, $N_{PLR}/P = 2$, $N_{CS}/P = 30$)	175 ± 7	0.34 ± 0.04	14.2 ± 0.4

3.2.3. Absence of cytotoxicity in the presence of non-targeted siRNA

The low cytotoxicity of CS-MSN is another parameter to be considered for a future biological application. In fact, we should ensure the safety of CS-MSN and show that the cell death effect is only due to the target siRNA. For that, a WST-1 viability test was carried out on MDA-MB-231 cells treated for different time periods (4–48 h) with CS-MSN prepared with different concentrations (12.5–100 nM) of a non-targeted control siRNA (Fig. 6). Non-treated cells and cells treated with H_2O_2 were used as controls. After 4 h and 24 h of treatment, the cell viability remained higher than 90% for all tested concentrations. A slight decrease of cell viability was observed at high CS-MSN concentration (100 nM) after 48 h of treatment. However, cell viability remained above 80% for this condition indicating a limited cytotoxic effect. This result proves the safety of the use of CS-MSN (up to 100 nM). Moreover, it also confirms that the previously observed decrease of cell fluorescence after siRNA transfection using CS-MSN (Fig. 3C) was not due to cellular mortality but it was a siRNA specific down regulation of GFP expression. The slight cytotoxicity observed at high siRNA concentration can be explained by the high density of positive charge of PLR. Thus, many studies highlighted the toxic effect of strongly cationic polymers (poly-lysine, poly-ethylenimine, poly-arginine, …) and showed that it is dose-dependent and it can be reduced by the association with chitosan or polyethylene glycol [33,34]. Herein, PLR is used at low N/P ratio and is associated to chitosan and PEGylated nanoparticles which provide to CS-MSN a high safety.

3.3. Transfection efficiency of CS-MSN

3.3.1. Determination of treatment and analysis times for an efficient siRNA transfection

To obtain an efficient siRNA transfection, it is important to consider i) a sufficient contact duration of nanovectors with cells, for their internalization (treatment time) and ii) a time period between treatment and analysis, long enough for the inhibition of the target protein (analysis time). To define these optimal conditions, first, MDA-MB-231/GFP cells were treated with CS-MSN prepared with anti-GFP siRNA for different treatment times (30 min – 72 h) and then analyzed after 72 h by flow cytometry. The GFP down regulation efficiency increased up to 4 h of contact between CS-MSN and cells. After 72 h of treatment, the down regulation efficiency is similar to that of 4 h (Fig. 7A), demonstrating the quick internalization of CS-MSN into cells. This result was confirmed by the analysis of the cyanine 5.5 fluorescence of CS-FNP. Indeed, after 4 h of treatment with CS-MSN, all cells express cyanine 5.5 fluorescence, which indicates the internalization of CS-MSN by MDA-

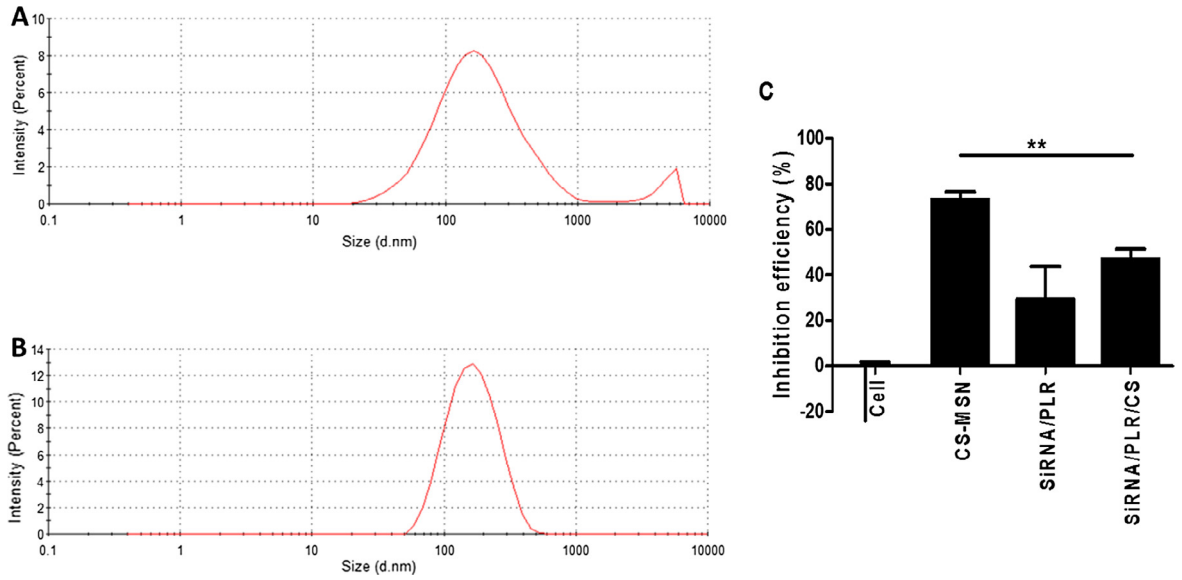

Fig. 4. Implication of CS-FNP in the CS-MSN formulation (A) Size distribution profile of complexes prepared with siRNA, PLR at $N_{PLR}/P = 2$ and Cs at $N_{CS}/P = 30$ measured by DLS. (B) Size distribution profile of CS-MSN prepared with CS-FNP (MR = 10), siRNA, PLR at $N_{PLR}/P = 2$ and Cs at $N_{CS}/P = 30$ measured by DLS. (C) Down regulation efficiency of GFP fluorescence in MDA-MB-231/GFP cells treated with CS-MSN (MR = 10, $N_{PLR}/P = 2$ and $N_{CS}/P = 30$), siRNA/PLR ($N_{PLR}/P = 2$) and siRNA/PLR/Cs complexes ($N_{PLR}/P = 2$, $N_{CS}/P = 30$).

MB-231 cancer cells (Fig. 7B). In a second stage, MDA-MB-231/GFP cells were treated for 4 h with CS-MSN and analyzed after different analysis time (24–72 h) using flow cytometry. The inhibition of the GFP expression in cells was more pronounced after 72 h than after 24 or 48 h (Fig. 7C). This indicates that even if the internalization of CS-MSN was fast, the inhibition of protein expression required more time (72 h). This relatively slow action of CS-MSN could be explained by the time needed to reach cytoplasm (intracellular trafficking and endosomal escape), for RNA interference mechanism and especially for the degradation of already produced GFP in target cells (half-life time of GFP). In fact, the GFP protein is known by its stability in cells which explain its large use as reporter in gene expression. It was reported that the stability of GFP depends highly on many factors like cell line and culturing conditions [35,36]. For the following experiments on MDA-MB-231 cells, the treatment time with CS-MSN and the analysis time by flow cytometry were fixed at 4 h and 72 h, respectively.

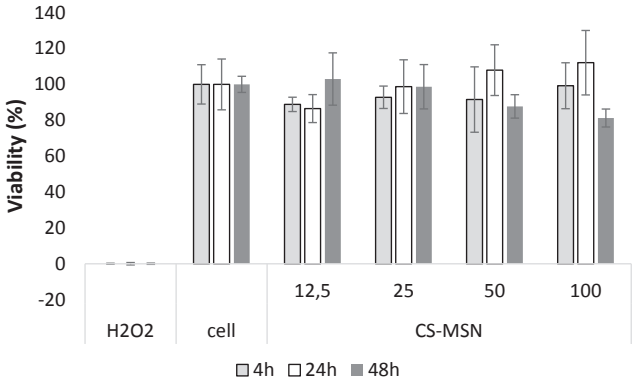

Fig. 6. Cellular viability of breast cancer cells treated for different time periods (4–48 h) with CS-MSN prepared with different concentrations (12.5–100 nM) of a non-targeted control siRNA.

3.3.2. Comparison of the transfection efficiency of CS-MSN with that of oligofectamine™

The last step of the proof-of-concept is to check that the transfection efficiency of CS-MSN is at least comparable to that of a commercial transfection agent, such as Oligofectamine™. Therefore, cells were treated with CS-MSN prepared with anti-GFP siRNA (siGFP) and the fluorescence intensity was measured using flow cytometry. Non-treated cells, Oligofectamine™-siRNA complexes and non-targeted vectorized siRNA (siCtrl) were used as controls (Fig. 8). With the non-targeted siRNA, transfection efficiency was comparable to non-treated cells independently of the nanovector (CS-MSN, Oligofectamine™-siRNA complexes). However, in presence of siGFP, the GFP down regulation efficiency of cells treated with CS-MSN (73 ± 3%) was significantly

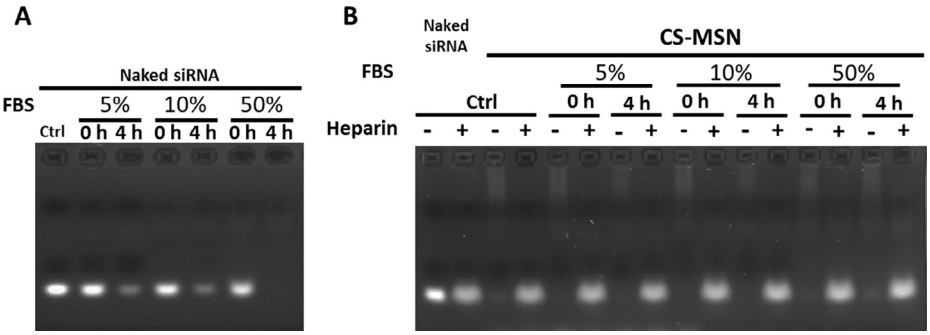

Fig. 5. Gel retardation assay to monitor siRNA degradation after incubation with serum. (A) Naked siRNA in water (Ctrl) or cell culture medium with FBS (5–50%). (B) Naked siRNA or CS-MSN in water (Ctrl) and CS-MSN in cell culture medium with FBS (5–50%), with (+) or without (−) heparin.

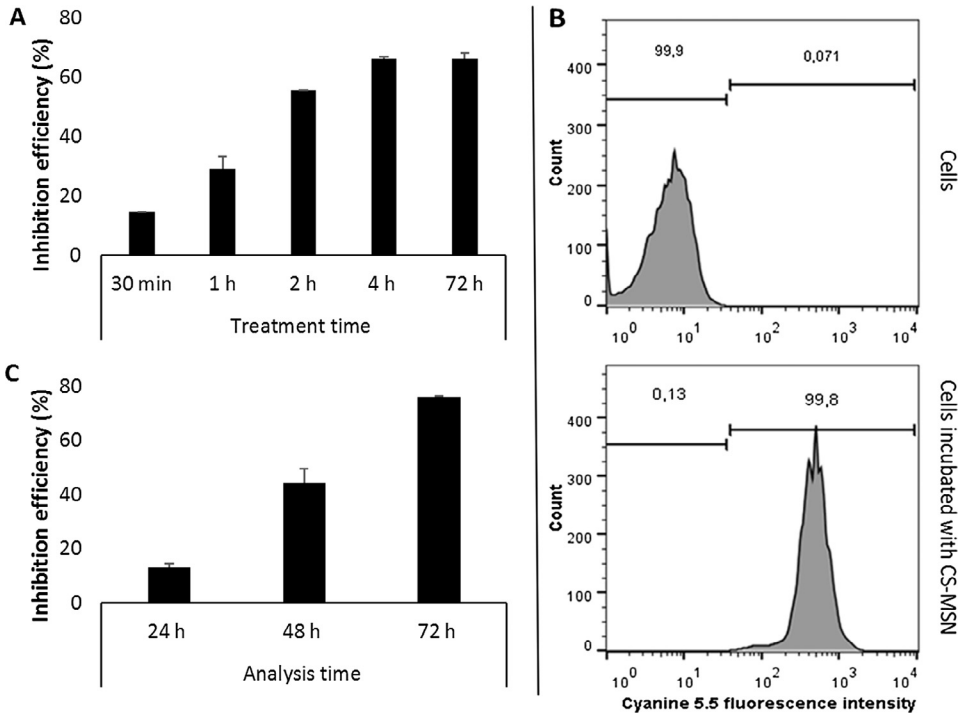

Fig. 7. Determination of treatment and analysis times for an efficient siRNA transfection in MDA-MB-231 cells. (A) Inhibition efficiency of GFP fluorescence with CS-MSN for different treatment times (30 min – 72 h). (B) Cyanine 5.5 fluorescence intensity of cells treated (lower figure) or not (upper figure) with CS-MSN for 4 h. (C) Inhibition efficiency of GFP fluorescence with CS-MSN for different analysis times (24–72 h).

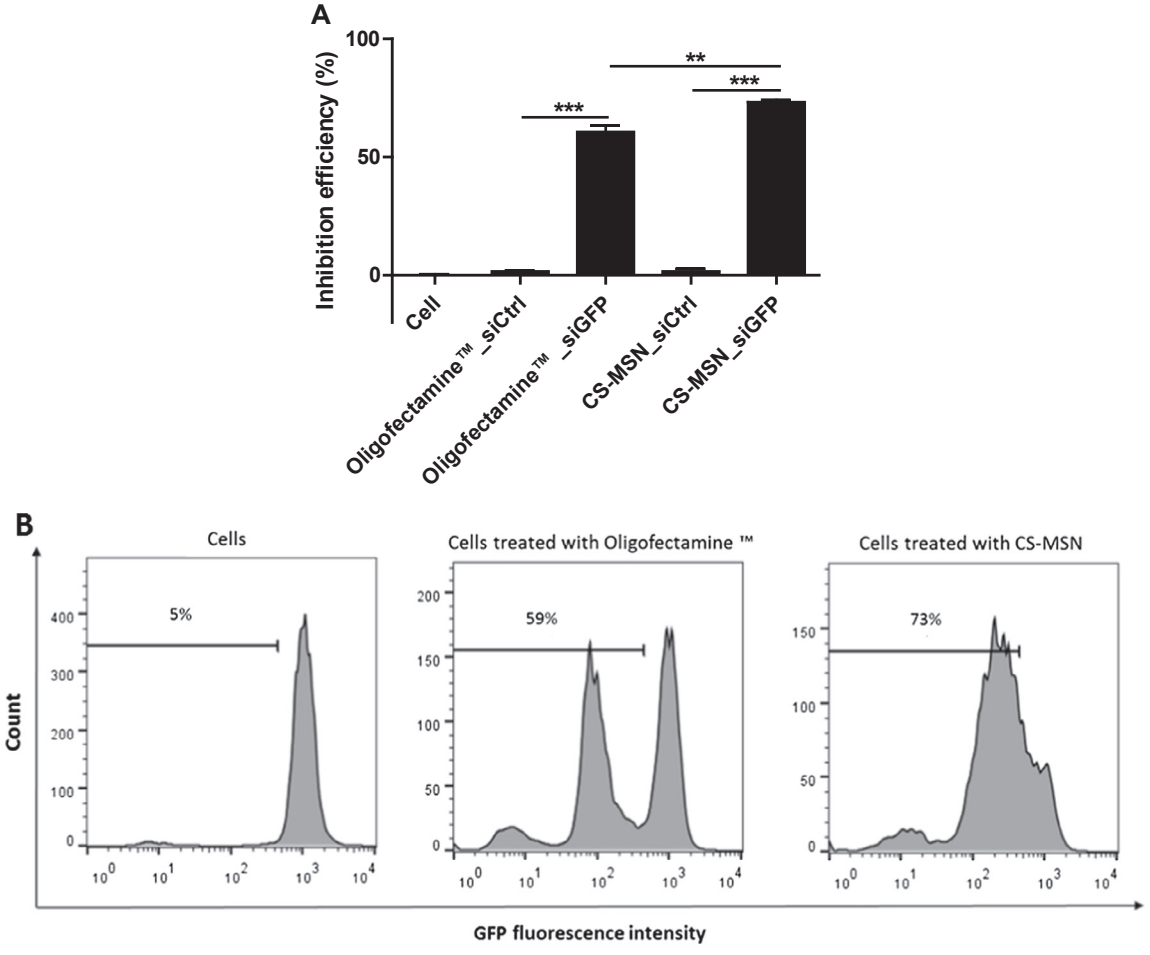

Fig. 8. Inhibition efficiency of GFP fluorescence with CS-MSN and Oligofectamine™-siRNA complexes. (A) Quantification of the down regulation efficiency of GFP fluorescent cells with Oligofectamine™-siRNA complexes and CS-MSN prepared with non-targeted siRNA (siCtrl) or anti-GFP siRNA (siGFP) (B) Fluorescence profiles obtained by Flow cytometer of untreated cells, cells treated with Oligofectamine™-siRNA complexes and cells treated with CS-MSN prepared with siGFP.

more pronounced than that of cells treated with Oligofectamine™ (59 ± 8%) ($p = 0.0026$) (Fig. 8A). That means, that the observed reduction in the GFP fluorescence intensity was due to the specific effect of the used siRNA. Fig. 8B shows differences in the fluorescence profile obtained by flow cytometry for cells treated with Oligofectamine™ and CS-MSN. Indeed, an efficient transfection is correlated either to a shift of the curve of the fluorescence to the left (CS-MSN) or to the appearance of a novel population of cells at lower fluorescence intensity (Oligofectamine™-siRNA complexes). The inhibition efficiencies of the transfected cell population were calculated and showed that Oligofectamine™ reduce the GFP expression by 91% in about 59% of cells without affecting the fluorescence of the other 41% of cells. For CS-MSN, the GFP expression was reduced by 82% in 73% of cells. These results indicate that even if our nanovector was a little bit less efficient in the transfected population than Oligofectamine™, it was able to affect more cells in an analogous manner. This explains the higher down regulation efficiency of GFP in treated cells with our nanovectors compared to Oligofectamine™. In the literature, the most effective siRNA nanovector have an efficiency between 60 and 88% [6,15,37] but, it is difficult to find the corresponding fluorescence profiles. These experiments prove the concept of CS-MSN as an efficient siRNA nanovector.

4. Conclusion

In view of a future application in theranosis of triple negative breast cancer, we successfully developed a novel siRNA delivery nanosystem, CS-MSN, which is based on PEGylated SPION functionalized with the cell-penetrating peptide gH625. The polymers poly-L-arginine and chitosan were added to the formulation to complex siRNA and to efficiently transfect breast cancer cells. CS-MSN exhibit a high ability to complex and protect siRNA against degradation in complete cell culture medium containing up to 50% of serum. In addition, CS-MSN showed a fast internalization (4 h) and a high siRNA transfection efficiency (73 ± 3%) in MDA-MB-231 cancer cells, while remaining non-toxic using a control siRNA at concentrations up to 100 nM. In contrast to Oligofectamine™, CS-MSN transfected almost all MDA-MB-231 cells with siRNA anti-GFP. Although CS-MSN were optimized using a model siRNA, they can be loaded with any siRNA sequence and thus are expected to allow a successful silencing of anti-apoptotic genes and oncogenes. The next step of this work will be the investigation of the role of the cell-penetrating peptide gH625 in the intracellular trafficking of CS-MSN and the *in vivo* application in a triple negative breast cancer mouse model.

Acknowledgments

This work was funded by the “Région Centre-Val de Loire” (MATURE Project) and supported by the “Cancéropôle Grand Ouest”. We thank Isabelle Dimier-Poisson, Nathalie Moire and Zineb Lakhrif (UMR INRA 1282, team of “Infectiologie et Santé Publique”, University of Tours) for their help with flow cytometry experiments.

Conflict of interest

The authors declare that they have no conflict of interest.

Appendix A. Supplementary material

Supplementary data associated with this article can be found, in the online version, at https://doi.org/10.1016/j.ejpb.2018.07.024.

References

[1] R. Venkitaraman, Triple-negative/basal-like breast cancer: clinical, pathologic and molecular features, Expert Rev. Anticancer Ther. 10 (2010) 199–207, https://doi.org/10.1586/era.09.189.
[2] E.A. Rakha, M.E. El-Sayed, A.R. Green, A.H.S. Lee, J.F. Robertson, I.O. Ellis, Prognostic markers in triple-negative breast cancer, Cancer 109 (2007) 25–32, https://doi.org/10.1002/cncr.22381.
[3] M. Kalimutho, K. Parsons, D. Mittal, J.A. López, S. Srihari, K.K. Khanna, Targeted therapies for triple-negative breast cancer: combating a stubborn disease, Trends Pharmacol. Sci. 36 (2015) 822–846, https://doi.org/10.1016/j.tips.2015.08.009.
[4] P. Guruprasath, J. Kim, G.R. Gunassekaran, L. Chi, S. Kim, R.-W. Park, S.-H. Kim, M.-C. Baek, S.M. Bae, S.-Y. Kim, D.-K. Kim, I.-K. Park, W.-J. Kim, B. Lee, Interleukin-4 receptor-targeted delivery of Bcl-xL siRNA sensitizes tumors to chemotherapy and inhibits tumor growth, Biomaterials 142 (2017) 101–111, https://doi.org/10.1016/j.biomaterials.2017.07.024.
[5] H. Jaganathan, S. Mitra, S. Srinivasan, B. Dave, B. Godin, Design and in vitro evaluation of layer by layer siRNA nanovectors targeting breast tumor initiating cells, PLOS One 9 (2014) e91986, https://doi.org/10.1371/journal.pone.0091986.
[6] T.A. Werfel, M.A. Jackson, T.E. Kavanaugh, K.C. Kirkbride, M. Miteva, T.D. Giorgio, C. Duvall, Combinatorial optimization of PEG architecture and hydrophobic content improves ternary siRNA polyplex stability, pharmacokinetics, and potency in vivo, J. Control. Release 255 (2017) 12–26, https://doi.org/10.1016/j.jconrel.2017.03.389.
[7] A. de Fougerolles, H.-P. Vornlocher, J. Maraganore, J. Lieberman, Interfering with disease: a progress report on siRNA-based therapeutics, Nat. Rev. Drug Discov. 6 (2007) 443–453, https://doi.org/10.1038/nrd2310.
[8] G. Meister, T. Tuschl, Mechanisms of gene silencing by double-stranded RNA, Nature (2004), https://doi.org/10.1038/nature02873.
[9] D. Haussecker, Current issues of RNAi therapeutics delivery and development, J. Control. Release 195 (2014) 49–54, https://doi.org/10.1016/j.jconrel.2014.07.056.
[10] M. Videira, A. Arranja, D. Rafael, R. Gaspar, Preclinical development of siRNA therapeutics: towards the match between fundamental science and engineered systems, Nanomed. Nanotechnol. Biol. Med. 10 (2014) 689–702, https://doi.org/10.1016/j.nano.2013.11.018.
[11] M. Ferrari, T. Sun, H. Shen, Nanovector delivery of siRNA for cancer therapy, Cancer Gene Ther. 19 (2012), https://doi.org/10.1038/cgt.2012.22.
[12] P. Resnier, T. Montier, V. Mathieu, J.-P. Benoit, C. Passirani, A review of the current status of siRNA nanomedicines in the treatment of cancer, Biomaterials 34 (2013) 6429–6443, https://doi.org/10.1016/j.biomaterials.2013.04.060.
[13] A. Carvalho, M.B.F. Martins, M.L. Corvo, G. Feio, Enhanced contrast efficiency in MRI by PEGylated magnetoliposomes loaded with PEGylated SPION: effect of SPION coating and micro-environment, Mater. Sci. Eng., C 43 (2014) 521–526, https://doi.org/10.1016/j.msec.2014.07.055.
[14] H. Mok, O. Veiseh, C. Fang, F.M. Kievit, F.Y. Wang, J.O. Park, M. Zhang, pH-sensitive siRNA nanovector for targeted gene silencing and cytotoxic effect in cancer cells, Mol. Pharm. 7 (2010) 1930–1939, https://doi.org/10.1021/mp100221h.
[15] O. Veiseh, F.M. Kievit, C. Fang, N. Mu, S. Jana, M.C. Leung, H. Mok, R.G. Ellenbogen, J.O. Park, M. Zhang, Chlorotoxin bound magnetic nanovector tailored for cancer cell targeting, imaging, and siRNA delivery, Biomaterials 31 (2010) 8032–8042, https://doi.org/10.1016/j.biomaterials.2010.07.016.
[16] O. Veiseh, F.M. Kievit, H. Mok, J. Ayesh, C. Clark, C. Fang, M. Leung, H. Arami, J.O. Park, M. Zhang, Cell transcytosing poly-arginine coated magnetic nanovector for safe and effective siRNA delivery, Biomaterials 32 (2011) 5717–5725, https://doi.org/10.1016/j.biomaterials.2011.04.039.
[17] E. Perillo, K. Hervé-Aubert, E. Allard-Vannier, A. Falanga, S. Galdiero, I. Chourpa, Synthesis and in vitro evaluation of fluorescent and magnetic nanoparticles functionalized with a cell penetrating peptide for cancer theranosis, J. Colloid Interf. Sci. 499 (2017) 209–217, https://doi.org/10.1016/j.jcis.2017.03.106.
[18] A.S. Hoffman, S.H. Pun, B.2 – Pegylation of drugs and nanocarriers, Biomater. Sci. third ed., Academic Press, 2013, p. 1028, , https://doi.org/10.1016/B978-0-08-087780-8.00090-5.
[19] D. Vllasaliu, R. Fowler, S. Stolnik, PEGylated nanomedicines: recent progress and remaining concerns, Expert Opin. Drug Deliv. 11 (2014) 139–154, https://doi.org/10.1517/17425247.2014.866651.
[20] S. Galdiero, A. Falanga, G. Morelli, M. Galdiero, gH625: a milestone in understanding the many roles of membranotropic peptides, Biochim. Biophys. Acta BBA – Biomembr. 2015 (1848) 16–25, https://doi.org/10.1016/j.bbamem.2014.10.006.
[21] M.S. Huh, S.-Y. Lee, S. Park, S. Lee, H. Chung, S. Lee, Y. Choi, Y.-K. Oh, J.H. Park, S.Y. Jeong, K. Choi, K. Kim, I.C. Kwon, Tumor-homing glycol chitosan/polyethylenimine nanoparticles for the systemic delivery of siRNA in tumor-bearing mice, J. Control. Release 144 (2010) 134–143, https://doi.org/10.1016/j.jconrel.2010.02.023.
[22] P. Sun, W. Huang, M. Jin, Q. Wang, B. Fan, L. Kang, Z. Gao, Chitosan-based nanoparticles for survivin targeted siRNA delivery in breast tumor therapy and preventing its metastasis, Int. J. Nanomed. 11 (2016) 4931–4945, https://doi.org/10.2147/IJN.S105427.
[23] M. Dominska, D.M. Dykxhoorn, Breaking down the barriers: siRNA delivery and endosome escape, J. Cell Sci. 123 (2010) 1183–1189, https://doi.org/10.1242/jcs.066399.
[24] J.J. Wang, Z.W. Zeng, R.Z. Xiao, T. Xie, G.L. Zhou, X.R. Zhan, S.L. Wang, Recent advances of chitosan nanoparticles as drug carriers, Int. J. Nanomed. 6 (2011) 765–774, https://doi.org/10.2147/IJN.S17296.
[25] Z.-X. Zhao, S.-Y. Gao, J.-C. Wang, C.-J. Chen, E.-Y. Zhao, W.-J. Hou, Q. Feng, L.-Y. Gao, X.-Y. Liu, L.-R. Zhang, Q. Zhang, Self-assembly nanomicelles based on cationic mPEG-PLA-b-Polyarginine(R15) triblock copolymer for siRNA delivery, Biomaterials 33 (2012) 6793–6807, https://doi.org/10.1016/j.biomaterials.2012.05.067.
[26] S. David, H. Marchais, D. Bedin, I. Chourpa, Modelling the response surface to

predict the hydrodynamic diameters of theranostic magnetic siRNA nanovectors, Int. J. Pharm. 478 (2015) 409–415, https://doi.org/10.1016/j.ijpharm.2014.11.061.
[27] J.C. Fernandes, X. Qiu, F.M. Winnik, M. Benderdour, X. Zhang, K. Dai, Q. Shi, Low molecular weight chitosan conjugated with folate for siRNA delivery in vitro: optimization studies, Int. J. Nanomed. 7 (2012) 5833–5845, https://doi.org/10.2147/IJN.S35567.
[28] N. Hoshyar, S. Gray, H. Han, G. Bao, The effect of nanoparticle size on in vivo pharmacokinetics and cellular interaction, Nanomedicine 11 (2016) 673–692, https://doi.org/10.2217/nnm.16.5.
[29] X. Liu, N. Huang, H. Li, Q. Jin, J. Ji, Surface and size effects on cell interaction of gold nanoparticles with both phagocytic and nonphagocytic cells, Langmuir 29 (2013) 9138–9148, https://doi.org/10.1021/la401556k.
[30] T.F. Martens, K. Remaut, J. Demeester, S.C. De Smedt, K. Braeckmans, Intracellular delivery of nanomaterials: how to catch endosomal escape in the act, Nano Today 9 (2014) 344–364, https://doi.org/10.1016/j.nantod.2014.04.011.
[31] S. Al-Qadi, A. Grenha, C. Remuñán-López, Chitosan and its derivatives as nanocarriers for siRNA delivery, J. Drug Deliv. Sci. Technol. 22 (2012) 29–42.
[32] X. Liu, K.A. Howard, M. Dong, M.Ø. Andersen, U.L. Rahbek, M.G. Johnsen, O.C. Hansen, F. Besenbacher, J. Kjems, The influence of polymeric properties on chitosan/siRNA nanoparticle formulation and gene silencing, Biomaterials 28 (2007) 1280–1288, https://doi.org/10.1016/j.biomaterials.2006.11.004.
[33] H. Lv, S. Zhang, B. Wang, S. Cui, J. Yan, Toxicity of cationic lipids and cationic polymers in gene delivery, J. Control. Release Off. J. Control. Release Soc. 114 (2006) 100–109, https://doi.org/10.1016/j.jconrel.2006.04.014.
[34] M.S. Shim, Y.J. Kwon, Efficient and targeted delivery of siRNA in vivo, FEBS J. 277 (2010) 4814–4827, https://doi.org/10.1111/j.1742-4658.2010.07904.x.
[35] P. Corish, C. Tyler-Smith, Attenuation of green fluorescent protein half-life in mammalian cells, Protein Eng. 12 (1999) 1035–1040.
[36] X. Li, X. Zhao, Y. Fang, X. Jiang, T. Duong, C. Fan, C.-C. Huang, S.R. Kain, Generation of destabilized green fluorescent protein as a transcription reporter, J. Biol. Chem. 273 (1998) 34970–34975, https://doi.org/10.1074/jbc.273.52.34970.
[37] Y. Ding, Y. Wang, J. Zhou, X. Gu, W. Wang, C. Liu, X. Bao, C. Wang, Y. Li, Q. Zhang, Direct cytosolic siRNA delivery by reconstituted high density lipoprotein for target-specific therapy of tumor angiogenesis, Biomaterials 35 (2014) 7214–7227, https://doi.org/10.1016/j.biomaterials.2014.05.009.